Enhanced saturable absorption of MoS_2 black phosphorus composite in 2 μm passively Q-switched Tm: YAP laser

Yang Xue (薛 杨)[1], Zhenda Xie (谢臻达)[2], Zhilin Ye (叶志霖)[1], Xiaopeng Hu (胡小鹏)[1,3], Jinlong Xu (徐金龙)[2,*], and Han Zhang (张 晗)[4]

[1]*National Laboratory of Solid State Microstructures, Nanjing University, Nanjing 210093, China*
[2]*School of Electronic Science and Engineering, Nanjing University, Nanjing 210093, China*
[3]*E-mail: xphu@nju.edu.cn*
[4]*College of Optoelectronic Engineering, Shenzhen University, Shenzhen 518060, China*
**Corresponding author: longno.2@163.com*

Received August 30, 2017; accepted October 20, 2017; posted online December 26, 2017

We report the fabrication of an MoS_2 black phosphorus (BP) composite saturable absorber by liquid phase exfoliation and the spin-coating method and further exploitation to build a 2 μm passively Q-switched Tm:YAP laser. Such a composite based Q-switched laser with a duration of 488 ns and corresponding peak power of 85.9 W is obtained, which shows an improved saturable absorption effect than that of single MoS_2 (616 ns, 68.7 W) and BP (932 ns, 22.4 W). The results indicate that simple and reasonable fabrication of the vertical composite from two-dimensional atomic layer materials opens up the possibility to create an unprecedented saturable absorber with exciting properties.

OCIS codes: 140.3540, 160.4236.
doi: 10.3788/COL201816.020018.

Tm^{3+} solid-state Q-switched lasers operating around 2 μm wavelength with short pulse duration and high peak power have important applications in many fields, such as laser radar[1], laser surgery[2], the pump source of a mid-infrared optical parametric oscillator (OPO)[3], etc. Active Q-switching based on acousto-optic[4] or electro-optic[5] modulators and passive Q-switching based on saturable absorbers (SAs) are two of the most commonly used methods to acquire a 2 μm pulsed laser. Compared with the active Q-switching technique, a more compact and lower cost structure make passive Q-switching a reasonable method for the generation of laser pulses within pulse durations from microseconds to picoseconds. Among such a passively Q-switched lasers, one of the key components is SA. The classical SAs for the 2 μm region are Cr^{4+}-doped crystals, such as Cr:ZnS[6] and Cr:ZnSe[7]. But, the low Cr-doping level, limited by the lattice defect induced from doping ions, usually needs a long crystal length of several millimeters to achieve sufficient absorption modulation. Thus, it further restricts the volume of the pulsed laser and even the development of a micro pulsed laser, such as a waveguide laser, semiconductor laser, and nanowire laser.

In recent years, because of the unique properties of an ultrathin layered structure, two-dimensional (2D) materials attract more and more attention for their potential applications in miniature optoelectronic devices. Many 2D materials, represented by graphene, consisting of an atom-thickness layered structure bonded by van der Waals forces, possess wideband absorption and a high thermal-induced damage threshold and, thus, have been widely proved as excellent SAs for near-mid-infrared Q-switched and mode-locked lasers[8,9]. Recently, several new classes of 2D materials that go beyond graphene have been investigated and developed, including a topological insulator[10], MoS_2[11,12], and black phosphorus (BP)[13,14]. Different from graphene, which has a zero band-gap, multilayer MoS_2 and any number layer BP own layer number dependent direct band-gaps. Up till now, both MoS_2 and BP have shown their progress potential as passive Q-switches at a 2 μm wavelength[15–18]. Moreover, the combination of MoS_2 and BP also has been recently investigated and employed for a near-infrared photodetector[19,20]. But, so far, there have been no reports of a passively Q-switched 2 μm laser by employing the composite of MoS_2 and BP, to the best of our knowledge. Therefore, whether the performance of the composite of these two materials has advantages over single MoS_2 or BP as a 2 μm passive Q-switch is still unclear.

In this Letter, passively Q-switched pulled lasers based on MoS_2, BP, and their composite were successfully achieved in a compact Tm:YAP laser, separately. Stable Q-switched pulse trains with durations of 616, 932, and 488 ns and repetition frequencies of 73, 110, and 86 kHz were separately obtained when the corresponding average powers reached 3.1, 2.3, and 3.6 W. The results indicate a better performance of the MoS_2–BP composite compared with an MoS_2 and BP single SA in the Tm:YAP laser.

The MoS_2 and BP nanosheets were prepared using the liquid phase exfoliation method[21]. Powder MoS_2 (or BP) was sufficiently dispersed in anhydrous alcohol (or NMP) by magnetic stirring. Followed by ultrasonic exfoliation for several hours and extraction by low speed centrifugation, two dispersions of MoS_2 and BP nanosheets were obtained, respectively. The corresponding microcosmic

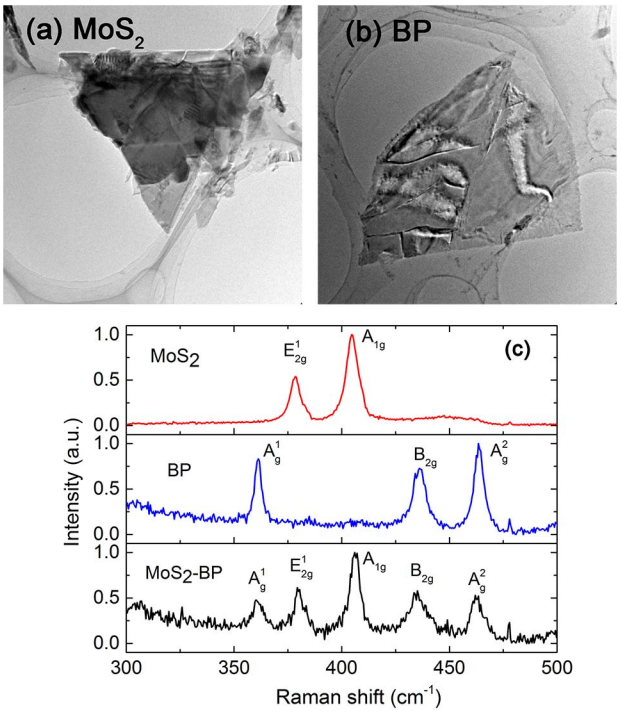

Fig. 1. TEM images of the prepared (a) MoS_2 and (b) BP nanosheets. (c) Characteristics of Raman spectra of a few layered MoS_2, BP, and MoS_2–BP composite.

pattern of the samples recorded by transmission electron microscopy (TEM) images is shown in Figs. 1(a) and 1(b). The prepared MoS_2 and BP nanosheets were separately spin-coated on two 2 μm output couplers to form SA mirrors (SAMs). Afterward, an MoS_2–BP SAM was fabricated by vertically spin-coating the two materials layer-by-layer.

A Raman measurement was also performed to verify the uniformity of the composite. Figure 1(c) shows the comparison of Raman characteristics of MoS_2, BP, and MoS_2–BP. The E^1_{2g} and A_{1g} modes were observed for MoS_2 and A^1_g, and B_{2g} and A^2_g modes for BP. For the MoS_2–BP composite, all five of these modes were observed, suggesting a good junction. Compared with typical Raman spectroscopy of bulk materials, these peak positions also indicate layered structures of our samples.

Then, the Z-scan measurement was employed to study the saturable absorption properties of these three SAs with a 70 ns, 1 kHz acoustic–optic Q-switched Tm:YAP laser as the signal source. The transmittances of different incident peak intensities were measured. Figure 2 shows the experimental data and fitting curves fitted by the following formula[22]:

$$T(I) = \frac{\Delta T}{1 + \frac{I}{I_{\text{sat}}}} + 1 - \alpha_{\text{ns}}, \tag{1}$$

where ΔT is the modulation depth, I is the pump peak intensity, I_{sat} is the saturable intensity, and α_{ns} is the non-saturable absorption. Extracted from the fitting

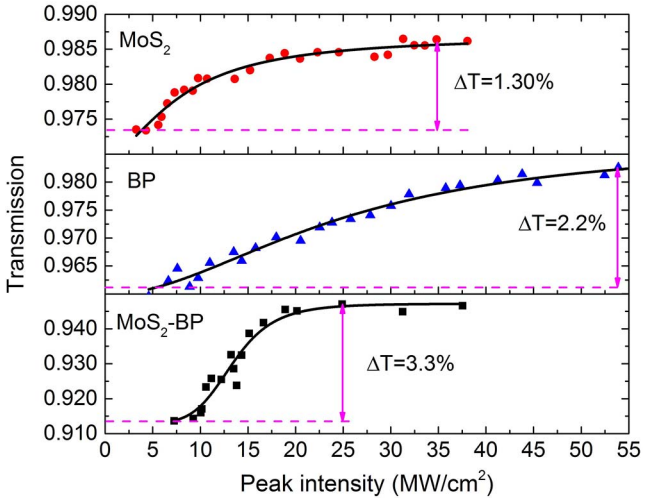

Fig. 2. Nonlinear transmissions of MoS_2, BP, and MoS_2–BP composite.

result, the modulation depths of the MoS_2, BP, and MoS_2–BP composite samples were, respectively, 1.3%, 2.2%, and 3.3% with corresponding saturable peak intensities of 7.90, 24.88, and 13.39 MW/cm^2. The improved modulation depth with a low saturable intensity of MoS_2–BP should be attributed to the multiple photon absorption channels and carrier lifetime extension that have been exhibited in a variety of photodetectors based on 2D material heterostructures[20,23,24].

We exploited the MoS_2, BP, and MoS_2–BP SAs to 2 μm laser pulse generation. As shown in Fig. 3, a compact plano-concave cavity pumped by a fiber coupled 795 nm laser diode (LD) was employed for our experiment. The total cavity length was fixed to 27 mm. An 8-mm-long a-cut 3 at% Tm:YAP was used as the gain medium, which was surrounded by a copper heat sink and cooled by circulating water at ~20°C. The input coupler M1 was a concave mirror with a curvature radius of 500 mm and coating films of 795 nm of high transmission and 2 μm of high reflection, while the output coupler M2 was a plain mirror with a transmission of 5% at 2 μm. Additionally, SAs were applied by spin-coating the prepared

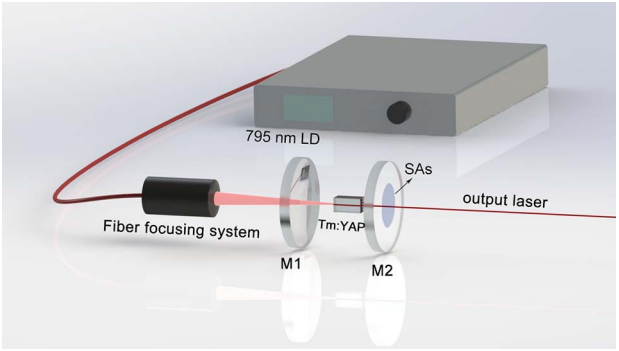

Fig. 3. Experimental setup of passively Q-switched Tm:YAP laser based on MoS_2, BP, and MoS_2–BP composite.

dispersions on the output coupler M2 instead of an additional insert element, which provided a lower cavity loss.

When the pump intensity increase exceeded the threshold, the laser beam was produced. The output laser pulse was detected by a mid-infrared photoelectric detector (Thorlabs PDA30G) and displayed on a digital oscilloscope (Tektronix DPO2024B). When the pump power was relatively low, the temporal pulse trains were unstable. At this pump level, the laser was working on continuous wave (CW) regime, and the unstable temporal pulse train was the result of self-Q-switching of Tm:YAP, which can also be observed without the SAs. Stable pulse trains could be observed when the absorbed pump power reached a certain level for different SAs. Typical temporal pulse trains of MoS_2, BP, and MoS_2–BP composite Q-switched lasers are exhibited in Fig. 4. The main diagram of each row is the screenshot of the oscilloscope when the time scale is set to 40 μm/div, and the attached diagram is the screenshot of a single pulse. Table 1 shows the comparison of the Q-switched output characteristics of these three SAs. In our experiment, the shortest pulse durations of 616, 932, and 488 ns for the MoS_2, BP, and MoS_2–BP composite were obtained, separately, under the corresponding average output powers of 3.1, 2.3, and 3.6 W and repetition frequencies of 73, 110, and 86 kHz. Furthermore, the calculated peak powers reached correspond to

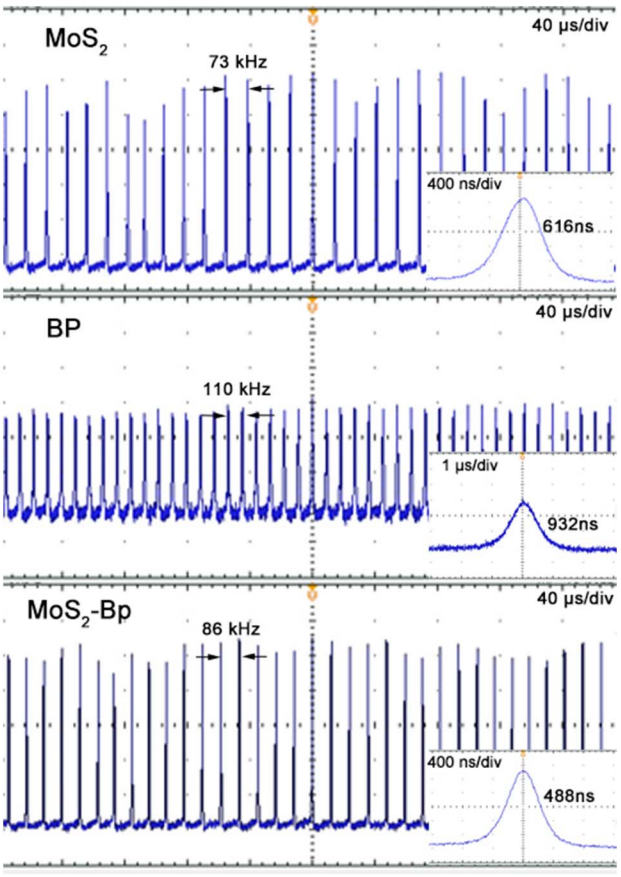

Fig. 4. Typical temporal pulse trains of Q-switched lasers based on (a) MoS_2, (b) BP, and (c) MoS_2–BP composite.

Table 1. Q-switched Output Characteristics of Three SAs

Parameter	MoS_2	BP	MoS2–BP
Pulse duration (ns)	616	932	488
Repetition frequency (kHz)	73	110	86
Average power (W)	3.1	2.3	3.6
Peak power (W)	68.7	22.4	85.9
Per-pulse energy (μJ)	42.5	20.9	41.8

68.7, 22.4, and 85.9 W, respectively. Figure 5 exhibits the variations of pulse durations and repetition frequencies for different SAs with absorbed pump power. As shown in Fig. 5, the pulse durations decrease with the pump power, but the repetition frequencies change at random when the absorbed pump power is above 8 W. This phenomenon should be attributed to the unsteady state of saturable absorption caused by the strong thermal expansion and thermal stress in the relaxation processes of SAs under a high pump level. Figure 6 shows the dependence of the average power of the output laser with absorbed pump power. From Fig. 6, the slope efficiencies of MoS_2, BP, and MoS_2–BP composite Q-switched lasers correspond to 24.6%, 21.7%, and 27.7%. The spectral characteristic of an MoS_2–BP-based Q-switched laser is described in Fig. 7. The central wavelength is located at 1993.1 nm, and the FWHM is about 1.5 nm. For single MoS_2 and BP Q-switched lasers, the central wavelengths and FWHM are not changed.

The results indicate that the composite of MoS_2 and BP has better performance as a passive Q-switch in a Tm:YAP laser compared with MoS_2 or BP single material. This advantage may be mainly attributed to the following two aspects. On one hand, the combination of these two SAs will naturally enhance the absorption. The larger

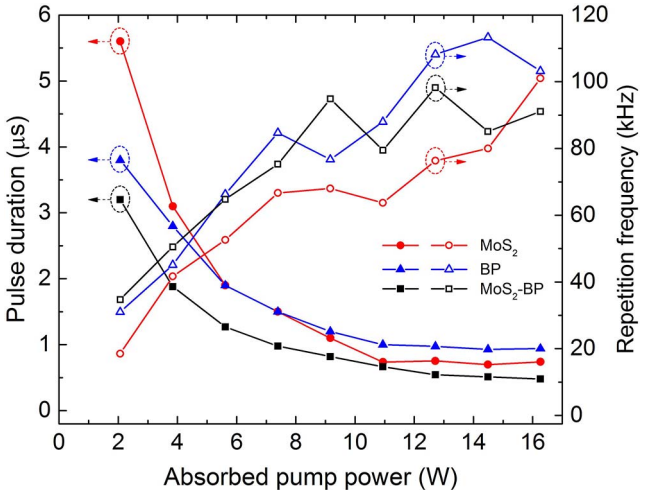

Fig. 5. (Color online) Variation of pulse duration and repetition frequency with absorbed pump power.

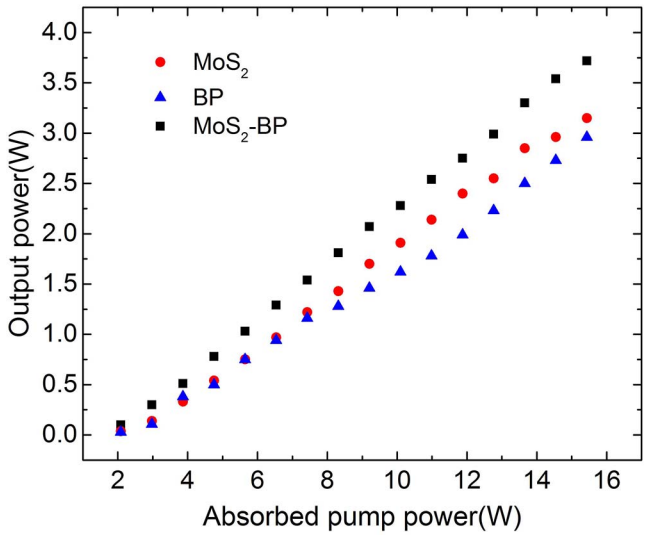

Fig. 6. (Color online) Output average powers of MoS_2, BP, and MoS_2–BP-based Q-switched lasers as functions of absorbed pump power.

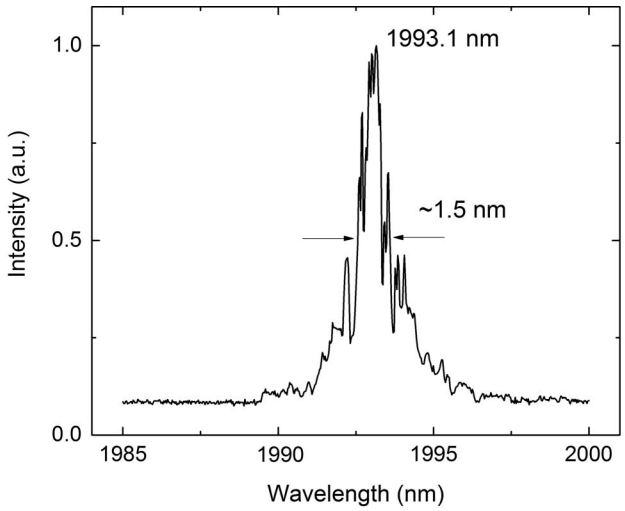

Fig. 7. Optical spectrum of MoS_2–BP Q-switched laser.

modulation depth of the MoS_2–BP composite showed in Fig. 2 can support this point. On the other hand, the direct band-gap of BP for all layer numbers makes up for the deficiency of the energy band structure of multilayer MoS_2 being indirect.

In conclusion, passively Q-switched Tm:YAP lasers based on MoS_2, BP, and MoS_2–BP composite are experimentally demonstrated separately. Stable Q-switched pulse trains at a 2 μm wavelength are acquired with several hundred nanoseconds pulse width and several tens of microjoules (μJ) of single pulse energy, and the results indicate that regardless of pulse width, average power, or peak power, the composite of MoS_2 and BP shows better performance than single MoS_2 or BP. For further study of the properties of composite of 2D materials in 2 μm Q-switching operation, we will attempt other 2D material combinations in our future work, such as MoS_2–WS_2, BP–WS_2, and so on.

This work was supported by the National Key R&D Program of China (No. 2017YFA0303700) and the National Natural Science Foundation of China (No. 11674171).

References

1. S. W. Henderson, P. J. M. Suni, C. P. Hale, M. Hannon, J. R. Magee, D. L. Bruns, and E. H. Yuen, IEEE Trans. Geosci. Remote Sens. **31**, 4 (1993).
2. N. M. Fried and K. E. Murray, J. Endourol. **19**, 25 (2005).
3. P. A. Budni, M. G. Knights, E. P. Chicklis, and K. L. Schepler, Opt. Lett. **33**, 315 (2008).
4. J. K. Jabczynski, W. Zendzian, J. Kwiatkowski, H. Jelínková, J. Šulc, and M. Němec, Laser Phys. Lett. **4**, 863 (2007).
5. A. F. El-Sherif and T. A. King, Opt. Commun. **218**, 337 (2003).
6. M. Segura, M. Kadankov, X. Mateos, M. C. Pujol, J. J. Carvajal, M. Aguiló, F. Díaz, U. Griebner, and V. Petrov, Opt. Express **20**, 3394 (2012).
7. T. Y. Tsai and M. Birnbaum, Appl. Opt. **40**, 6633 (2001).
8. J. L. Xu, X. L. Li, J. L. He, X. P. Hao, Y. Yang, Y. Z. Wu, S. D. Liu, and B. T. Zhang, Opt. Lett. **37**, 2652 (2012).
9. G. Q. Xie, J. Ma, P. Lv, W. L. Gao, P. Yuan, L. J. Qian, H. H. Yu, H. J. Zhang, J. Y. Wang, and D. Y. Tang, Opt. Mater. Express **2**, 878 (2012).
10. P. Tang, X. Zhang, C. J. Zhao, Y. Wang, H. Zhang, D. Y. Shen, S. C. Wen, D. Y. Tang, and D. Y. Fan, IEEE Photon. J **5**, 1500707 (2013).
11. S. X. Wang, H. H. Yu, H. J. Zhang, A. Z. Wang, M. W. Zhao, Y. X. Chen, L. M. Mei, and J. Y. Wang, Adv. Mater. **26**, 3538 (2014).
12. A. Alharbi, P. Zahl, and D. Shahrjerdi, Appl. Phys. Lett. **110**, 033503 (2017).
13. X. Ren, J. Zhou, X. Qi, Y. Liu, Z. Huang, Z. Li, Y. Ge, S. C. Dhanabalan, J. S. Ponraj, S. Wang, J. Zhong, and H. Zhang, Adv. Energy Mater. **7**, 1700396 (2017).
14. X. Ren, Z. Li, Z. Huang, D. Sang, H. Qiao, X. Qi, J. Li, J. Zhong, and H. Zhang, Adv. Funct. Mater. **27**, 1606834 (2017).
15. P. Ge, J. Liu, S. Jiang, Y. Xu, and B. Man, Photon. Res. **3**, 256 (2015).
16. C. Luan, X. Y. Zhang, K. J. Yang, J. Zhao, S. Z. Zhao, T. Li, W. C. Qiao, H. W. Chu, J. P. Qiao, J. Wang, L. H. Zheng, X. D. Xu, and J. Xu, IEEE J. Sel. Top. Quantum Electron. **23**, 66 (2017).
17. Z. Chu, J. Liu, Z. Guo, and H. Zhang, Opt. Mater. Express **6**, 2374 (2016).
18. Y. X. Xie, L. C. Kong, Z. P. Qin, G. Q. Xie, and J. Zhang, Opt. Eng. **55**, 081307 (2016).
19. Y. Deng, Z. Luo, N. J. Conrad, H. Liu, Y. Gong, S. Najmaei, P. M. Ajayan, J. Lou, X. Xu, and P. D. Ye, ACS Nano **8**, 8292 (2014).
20. L. Ye, H. Li, Z. F. Chen, and J. B. Xu, ACS Photon. **3**, 692 (2016).
21. P. Yasaei, B. Kumar, T. Foroozan, C. Wang, M. Asadi, D. Tuschel, J. E. Indacochea, R. F. Klie, and A. SalehiKhojin, Adv. Mater. **27**, 1887 (2015).
22. S. Wang, H. Yu, H. Zhang, A. Wang, M. Zhao, Y. Chen, L. Mei, and J. Wang, Adv. Mater. **26**, 3538 (2014).
23. W. J. Zhang, C. P. Chuu, J. K. Huang, C. H. Chen, M. L. Tsai, Y. H. Chang, C. T. Liang, Y. Z. Chen, Y. L. Chueh, J. H. He, M. Y. Chou, and L. J. Li, Sci. Rep. **4**, 3826 (2014).
24. Y. Liu, F. Wang, X. Wang, X. Wang, E. Flahaut, X. Liu, Y. Li, X. Wang, Y. Xu, Y. Shi, and R. Zhang, Nat. Commun. **6**, 8589 (2015).